Archives of Biochemistry and Biophysics 644 (2018) 17–28

Contents lists available at ScienceDirect

Archives of Biochemistry and Biophysics

journal homepage: www.elsevier.com/locate/yabbi

The primary cause of muscle disfunction associated with substitutions E240K and R244G in tropomyosin is aberrant behavior of tropomyosin and response of actin and myosin during ATPase cycle

Armen O. Simonyan[a,b], Vladimir V. Sirenko[a], Olga E. Karpicheva[a], Katarzyna Robaszkiewicz[c], Małgorzata Śliwinska[c], Joanna Moraczewska[c], Zoya I. Krutetskaya[b], Yurii S. Borovikov[a,*]

[a] Institute of Cytology of the Russian Academy of Sciences, Laboratory of Molecular Basis of Cell Motility, 4 Tikhoretsky Ave., 194064, Saint Petersburg, Russia
[b] Saint Petersburg State University, Faculty of Biology, Department of Biophysics, 7/9 Universitetskaya Emb., 199034, Saint Petersburg, Russia
[c] Kazimierz Wielki University in Bydgoszcz, Institute of Experimental Biology, Department of Biochemistry and Cell Biology, Ks. J. Poniatowski 12 Str., 85-671, Bydgoszcz, Poland

ARTICLE INFO

Keywords:
Tropomyosin
F-actin
Myosin
Troponin
Ghost muscle fibres
Congenital myopathies
Fluorescence polarization

ABSTRACT

Using the polarized photometry technique we have studied the effects of two amino acid replacements, E240K and R244G, in tropomyosin (Tpm1.1) on the position of Tpm1.1 on troponin-free actin filaments and the spatial arrangement of actin monomers and myosin heads at various mimicked stages of the ATPase cycle in the ghost muscle fibres. E240 and R244 are located in the C-terminal, seventh actin-binding period, in *f* and *b* positions of the coiled-coil heptapeptide repeat. Actin, Tpm1.1, and myosin subfragment-1 (S1) were fluorescently labeled: 1.5-IAEDANS was attached to actin and S1, 5-IAF was bound to Tpm1.1. The labeled proteins were incorporated in the ghost muscle fibres and changes in polarized fluorescence during the ATPase cycle have been measured. It was found that during the ATPase cycle both mutant tropomyosins occupied a position close to the inner domain of actin. The relative amount of the myosin heads in the strongly-bound conformations and of the switched on actin monomers increased at mimicking different stages of the ATPase cycle. This might be one of the reasons for muscle dysfunction in congenital fibre type disproportion caused by the substitutions E240K and R244G in tropomyosin.

1. Introduction

Tropomyosin is a coiled-coil actin-binding protein involved along with troponin complex in the regulation of actin-myosin interaction. According to current concepts, the regulation of actin-myosin interaction by tropomyosin occurs by three stages [1,2]. At low calcium, tropomyosin is located close to the outer domain of actin and together with troponin complex blocks the sites for strong myosin binding on actin ("Blocked" or "B-state"). Increasing calcium concentrations from 10^{-7} to 10^{-5} M in the sarcoplasm of skeletal muscle fibre leads to an azimuthal shift of tropomyosin strands towards the inner domain of actin, to the centre of actin filaments ("Closed" or "C-state"). This partially opens the sites for strong binding of myosin and in consequence myosin heads can bind not only weakly but also strongly to actin. This results in a further myosin-induced displacement of tropomyosin strands to the inner domain of actin ("M-state"), causing a cooperative activation of the filament and binding of a larger number of myosin heads [3]. In the absence of troponin complex the tropomyosin molecule is localized in the Apo-state position [4], which is near to the C-position [5,6]. In this state tropomyosin doesn't completely cover the myosin binding sites on actin and, as a result, myosin heads can bind to actin. It is a well known phenomenon that in the presence of TM myosin cooperatively switches the thin filament from the closed to open state. TM is therefore a dual regulator, which inhibits the actin-activated myosin ATPase at low myosin to actin ratios but activates it at high ratios.

To assess the functional role of tropomyosin as an actin-binding protein a number of mutagenesis studies have been performed (see rev. [7]). These studies have revealed the importance of individual amino acid residues in stabilization of the coiled-coil structure and the ability of the tropomyosin molecule to bind to actin. The structural data have also shown that the C-terminal region of tropomyosin splits apart to

Abbreviations used: 1,5-IAEDANS, N-(iodoacetaminoethyl)-1-naphthyl-amine-5-sulfonic acid; 5-IAF, 5-iodoacetamidofluorescein; TM-WT, wild type recombinant Tpm1.1; TM-E240K, Tpm1.1 carrying the substitution E240K; TM-R244G, Tpm1.1 carrying the substitution R244G

* Corresponding author.
E-mail address: borovikov@incras.ru (Y.S. Borovikov).

https://doi.org/10.1016/j.abb.2018.03.002
Received 26 June 2017; Received in revised form 16 February 2018; Accepted 2 March 2018
Available online 03 March 2018
0003-9861/

form a fork-like structure, which accommodates the N-terminus of the neighboring tropomyosin molecule in an end-to-end overlap. The specific structure of the overlap is thought to determine the position tropomyosin chains assume on the actin filament [8,9].

To date a large number of mutations in tropomyosin associated with human congenital myopathies have been identified. The most frequent myopathies are cases of nemaline myopathy (NM), congenital fibre type disproportion (CFTD), distal arthrogryposis (DA), and cap-disease (CD). The CFTD is a genetically heterogeneous disease which is manifested in fibre type 1 hypotrophy relative the type 2B fibres, contractures and muscle weakness. Most CFTD-causing mutations were found in *TPM3* gene encoding tropomyosin expressed in slow skeletal muscle (Tpm3.12). Among them are substitutions E241K and R245G located in the C-terminal domain of Tpm3.12 [10,11]. However, when introduced into *TPM1* gene the mutations impair *in vitro* functions of fast skeletal Tpm1.1 in a way that is consistent with the effects observed in myopathy patients [11]. This suggests that the regions affected by mutations share similar functions in both TM isoforms.

The main goal of the present study was to investigate the effect of two substitutions, E240K and R244G, in the recombinant tropomyosin of fast skeletal muscle (Tpm1.1) on changes in position of TM and the response of the myosin heads and actin to TM movement during the ATPase cycle. The substituted sites are equivalent to the sites of mutations found in Tpm3.12 of myopathy patients. Using the method of polarized fluorimetry we have investigated the effects of both substitutions in Tpm1.1 on the mobility of actin, myosin subfragment 1, and tropomyosin in the ghost fibres in the absence of troponin upon simulated different stages of the actomyosin ATPase cycle. It was found that TM-E240K and TM-R244G predominantly occupy the position, which is close to the inner domain of actin (nearby from M-position) and increase the amount of the myosin heads which are in the strong-binding states. Each mutation decreases the amplitude of the tilting of the myosin SH1 helix (or the myosin head) during the ATPase cycle, which indicates a reduction of the efficiency of the cross-bridge cycle in the muscle fibres. It was shown that Tpm1.1 with the substitutions inhibits the actomyosin ATPase activity stronger than the wild type tropomyosin. The results allow us to suggest that localization of tropomyosins' mutants near actin inner domain during the different states of the ATPase cycle and an abnormal response of actomyosin to tropomyosin movement could also take place in the case of Tpm3.12 carrying the same substitutions and, consequently, could be one of the reasons of muscle dysfunction development in affected patients.

2. Materials and methods

2.1. Preparation and labeling of proteins

Myosin was separated from mixed type skeletal muscles of rabbits as described by Margossian and Lowey [12]. Myosin subfragment-1 (S1) was prepared by treatment of the skeletal muscle myosin with α-chymotrypsin for 10 min at 25 °C according to Okamoto and Sekine [12]. Modification of the reactive residue Cys707 of S1 with 1,5-IAEDANS (Molecular Probes, actin-AEDANS) was carried out as described previously [13]. The degree of Cys707 modification was 0.90–0.95.

G-actin was isolated from the acetone powder of rabbit skeletal muscle with the use of Spudich and Watt method [14]. Actin was labeled at Cys374 with *N-(iodoacetaminoethyl)-1-naphthyl-amine-5-sulfonic acid* (1,5-IAEDANS, Molecular Probes, actin-AEDANS) by the following protocol. F-actin (2 mg/ml) was mixed with a 10-fold molar excess of 1,5-IAEDANS in 0.1 M KC1, 1 mM $MgCl_2$ and 20 mM Tris-HCl buffer, pH 7.0 at room temperature for 1 h. The reaction was terminated by the addition of 1 mM DTT (dithiothreitol). The solution was centrifuged at 100,000 × g at 20 °C for 1 h. The pellet was dissolved in K-Mg buffer (50 mM KCl, 2 mM $MgCl_2$, 2 mM DTT, and 10 mM Tris-HCl, pH 7.0) and dialyzed exhaustively against the same buffer solution. The concentration of labeled actin was determined from the absorbance at 595 nm using the Coomassie protein assay reagent. The absorption coefficient of 6100 $M^{-1}cm^{-1}$ at 336 nm for 1,5-IAEDANS bound to actin was used [14]. The labelling ratio was 0.9.

Recombinant wild type and mutant Tpm1.1 carrying E240K and R244G substitutions were expressed in BL21 (DE3) cells and purified as described before [15]. All tropomyosins had an extension of two additional amino acids (AlaSer), which compensated for the reduced affinity of recombinant non-acetylated skeletal TM to F-actin. TM labeling with 5-IAF (Sigma, the USA) at Cys190 was performed as described previously [16,17], producing a probe to protein molar ratio 0.8:1.

2.2. Preparation of ghost fibres

The experiments were performed at the animal care facility of the Institute of Cytology RAS. Adult male New Zealand white rabbits (3–4 kg) were killed by sodium pentobarbitone injection (200 mg/kg) in accordance with the official regulations of the community council on the use of laboratory animals, and the study was approved by the ethics committee for animal experiments. The psoas muscle was exposed ventrally and a bundle of about 100 fibres was gently separated from the muscle. The fibres were glycerinated using the method of Rome [18]. Ghost fibres were prepared by incubation of single glycerinated skeletal fibres for 1.5 h in 800 mM KCl, 1 mM $MgCl_2$, 10 mM ATP, 67 mM phosphate buffer, pH 7.0 [9]. Actin accounted for 80% of the overall protein content of the ghost fibres (Fig. 1).

Reconstruction of actin filaments with exogenous G-actin was performed according to the procedures described previously in detail. It has been shown that G-actin both modified with 1,5-IAEDANS and unmodified polymerizes in ghost muscle fibres equally well, through the formation of new filaments and the extension of existing actin filaments [19] The degree of incorporation (30–80%) had no effect on the conformational changes in actin induced by S1 [19].

S1 and TM were incorporated into the actin filaments by incubation of the fibre in a standard solution containing 50 mM KCl, 3 mM $MgCl_2$, 1 mM DTT, 10 mM Tris-HCl, pH 6.8, and the respective protein in concentration 1.0–2.5 mg/ml. The unbound proteins were washed out by incubation of the fibres in the same buffer devoid of proteins.

The effectiveness of reconstitution of the filaments in ghost muscle fibres used for fluorescent measurements was verified by SDS-PAGE. The fibres in the final preparations contained actin, S1, recombinant TM and Z-line proteins. The molar ratio of TM-WT or mutant TMs to actin was 1:6.5 (± 2) irrespectively of whether TMs were modified by 5-IAF or not. In the absence of nucleotides and in the presence of MgADP, MgAMP-PNP, and MgATP the molar ratios of S1 to actin were

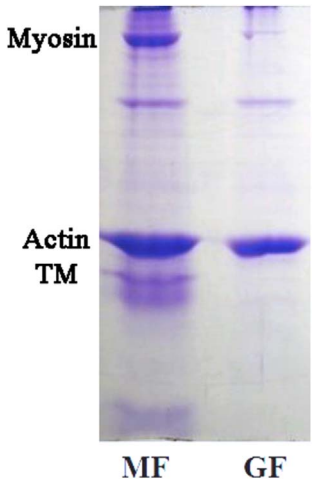

Fig. 1. SDS-PAGE of skinned muscle fibres (MF) and ghost fibres (GF). For each band 10–12 fibres were used. 12% PAA gel was used.

1:5 (± 2), 1:5 (± 2), 1:8 (± 2), and 1:14 (± 2), respectively.

2.3. ATPase activity measurements

The actomyosin ATPase activity has been analyzed at 22^0 by following inorganic phosphate release rate. The analysis was carried out in 96-well microtiter plates in a solution containing 12 mM Tris-HCl (pH 6.0), 2.5 mM $MgCl_2$, 5 mM KCl, 0.4 mM $CaCl_2$, and 2 mM DTT. The reaction was initiated by adding Mg-ATP to the final concentration 2 mM and terminated after 3 min. by adding 3.3% SDS and 30 mM EDTA. The amount of inorganic phosphate released was determined colorimetrically by the method described in Ref. [20].

2.4. Determination of tropomyosin affinity for F-actin

Tropomyosin binding to actin was studied by a cosedimentation assay as described earlier [21]. The assay samples were composed of 7 μM filamentous F-actin, 0.5 μM S1 and Tpm1.1 at concentrations varying from 0.25 to 4 μM in 12 mM Tris-HCl (pH 6.0), 2.5 mM $MgCl_2$, 5 mM KCl, 0.4 mM $CaCl_2$, 2 mM DTT and 2 mM ATP. F-actin and tropomyosins were mixed, incubated at room temperature for 0.5 h. S1 and ATP were added and the smaples were immediately ultracentrifuged for 1 h at 40,000 rpm in Beckman rotor 42.2. The composition of the proteins in pellets were examined on 10% SDS-PAGE. The gels were stained with Coomassie Blue, scanned and quantitated using EasyDens (Cortex Nova, Bydgoszcz, Poland) software. Fractional saturation of actin filaments with tropomyosin at each tropomyosin concentration was obtained by dividing the tropomyosin electrophoretic band density by actin density. The experimental points were fit in SigmaPlot 12.5 (Systat Software Inc.) to the following Hill equation:

$$v = n[TM]^{\alpha H}K_{50\%}/(1 + [TM]^{\alpha H}K_{50\%}{}^{\alpha H})$$

where v – fraction of tropomyosin bound to actin; n – fractional saturation of the filament with tropomyosin; [TM] – concentration of tropomyosin; $K_{50\%}$ – half maximal saturation; α^H – Hill cooperativity coefficient.

2.5. Polarized light measurements

Steady-state fluorescence polarization measurements on single ghost muscle fibres (GF) were made using a flow-through chamber and polarized fluorimeter [22]. The polarized fluorescence from 1,5-IAEDANS-labeled S1 and IAEDANS-labeled actin was excited at 407 ± 5 nm, and from 5-IAF-labeled tropomyosin, at 436 ± 5 nm and recorded at 500–600 nm. The intensities of four components of polarized fluorescence, $_{||}I_{||}$, $_{||}I_{\perp}$, $_{\perp}I_{\perp}$, and $_{\perp}I_{||}$, were detected by two photomultiplier tubes. The subscripts || and ⊥ designate the direction of polarization parallel and perpendicular to the fibre axis, the former denoting the direction of polarization of the incident light and the latter that of the emitted light. Fluorescence polarization ratios were defined as:

$$P|| = (_{||}I_{||} - {}_{||}I_{\perp})/(_{||}I_{||} + {}_{||}I_{\perp}) \text{ and } P\perp = (_{\perp}I_{\perp} - {}_{\perp}I_{||})/(_{\perp}I_{\perp} + {}_{\perp}I_{||}).$$

Fluorescent probes bound to the proteins in muscle fibre arrange in the highly ordered manner that results in the appearance of polarized fluorescence and allows us to determine the average orientation of the probes and their mobility. According to the helix plus isotropic model [22], the absorption and emission of light is accomplished by linear, completely anisotropic dipoles of absorption (A) and emission (E). The axes of dipoles of the ordered probes are arranged in a spiral along the surface of the cone, the axis of which coincides with the long axis of the thin filament. There are two populations of fluorophores in the muscle fibre – the population of randomly distributed fluorophores (N) oriented at the magic angle of 54.7°, and the population of fluorophores located in a spiral (1–N) at an angle not equal to 54.7°. Fluorophores with the magic angle 54.7° are not included in the population of the orderly oriented fluorophores (1–N), and are considered as randomly oriented (contributing to N).

The thin filament is flexible with the maximal angle of deviation from the fibre axis $\theta_{1/2}$ [30]. The values of Φ_A, Φ_E and $\sin^2\theta$ fit by mathematical analysis to give the best agreement with the observed values of the ratios $_{\perp}I_{\perp}/_{||}I_{||}$, $_{||}I_{\perp}/_{||}I_{||}$ and $_{\perp}I_{||}/_{||}I_{||}$ [22,23]. The number of completely disordered probes N indicates the mobility of the labeled protein. The character of the Φ_A and Φ_E changes coincides with each other, so the only one of these values is presented when analyzing the results.

We measured the position of the maximum of the fluorescence spectrum in all the experiments with an accuracy of 0.3 nm, and did not find any reliable shifts of the spectrum of the proteins modified by 5-IAF or 1,5-IAEDANS. Based on these data we concluded that the registered changes in polarized fluorescence reflected mainly the changes in orientation and mobility of the probe-containing areas of the proteins. In the study it is suggested that the changes in the values of Φ_E and $\theta_{1/2}$ contain qualitative information on a magnitude and direction of the spatial rearrangements of the proteins or their parts.

Measurements were carried out in solutions containing 1 mM DTT, 6.7 mM phosphate buffer, pH 7.0, in the absence or presence of 3 mM ADP, 16 mM AMP-PNP or 5 mM ATP. The concentration of $MgCl_2$ was 3 mM when experimental medium contained ADP or no nucleotides, 8 mM in the presence of ATP, and 18 mM in the presence of AMP-PNP [24].

The data were obtained from 6 to 8 fibres for each experiment (60–80 measurements). Statistically significant differences between two groups were determined using an unpaired Student's t-test, with significance defined as $P < 0.05$. The software (designed in our laboratory or Sigma Plot 11; System Software, San Jose, CA) intended for the analysis of polarized fluorescence provided the determination of the reliability of the obtained data.

3. Results

To understand the obtained results and their interpretation presented below, it is necessary to consider the following important points. The dipoles of the probes attached covalently to actin (Ac), myosin subfragment-1 (S1), and tropomyosin (TM) are set at the angles denoted as Φ_E to the axis of muscle fibre/thin filament as shown in Fig. 2A and B.

The scheme in Fig. 2A shows that 1,5-IAEDANS covalently bound to Cys707 of myosin S1 (S1-AEDANS) and 5-IAF covalently bound to Cys190 of tropomyosin are directed at the angle Φ_E (it has different value for each of the probes). When myosin head binds strongly or weakly to actin, the value of the angle Φ_E decreases or increases, respectively. Similarly, tropomyosin's azimuthal movement toward the centre (O-state) or the periphery (C-state) of F-actin leads to an increase or decrease of Φ_E, respectively (Fig. 2A). In fact, changes in the values of Φ_E related tothe tropomyosin movement cannot take place if changes in tropomyosin radius from thin filament axis do not occur. The model of F-actin-tropomyosin complex has shown that tropomyosin is bound to F-actin at a radius of 39 Å [25]. A comparison of atomic coordinates of tropomyosin and EM-reconstructions of F-actin-tropomyosin-troponin complex has shown that the radius is different in the absence and presence of calcium (from 40 to 42 Å [26]). It is likely that changes in the radius also occur in the absence of troponin and calcium, which are reflected in the changes of Φ_E. Finally, the switching of Ac-AEDANS from OFF to ON states leads to an increase in the value of Φ_E (Fig. 2B).

3.1. The effects of E240K and R244G substitutions in tropomyosin on the mobility and the flexibility of actin filaments

In line with our previously published data [27–29], the incorporation of IAEDANS-labeled actin into ghost fibres (Ac-AEDANS) initiated

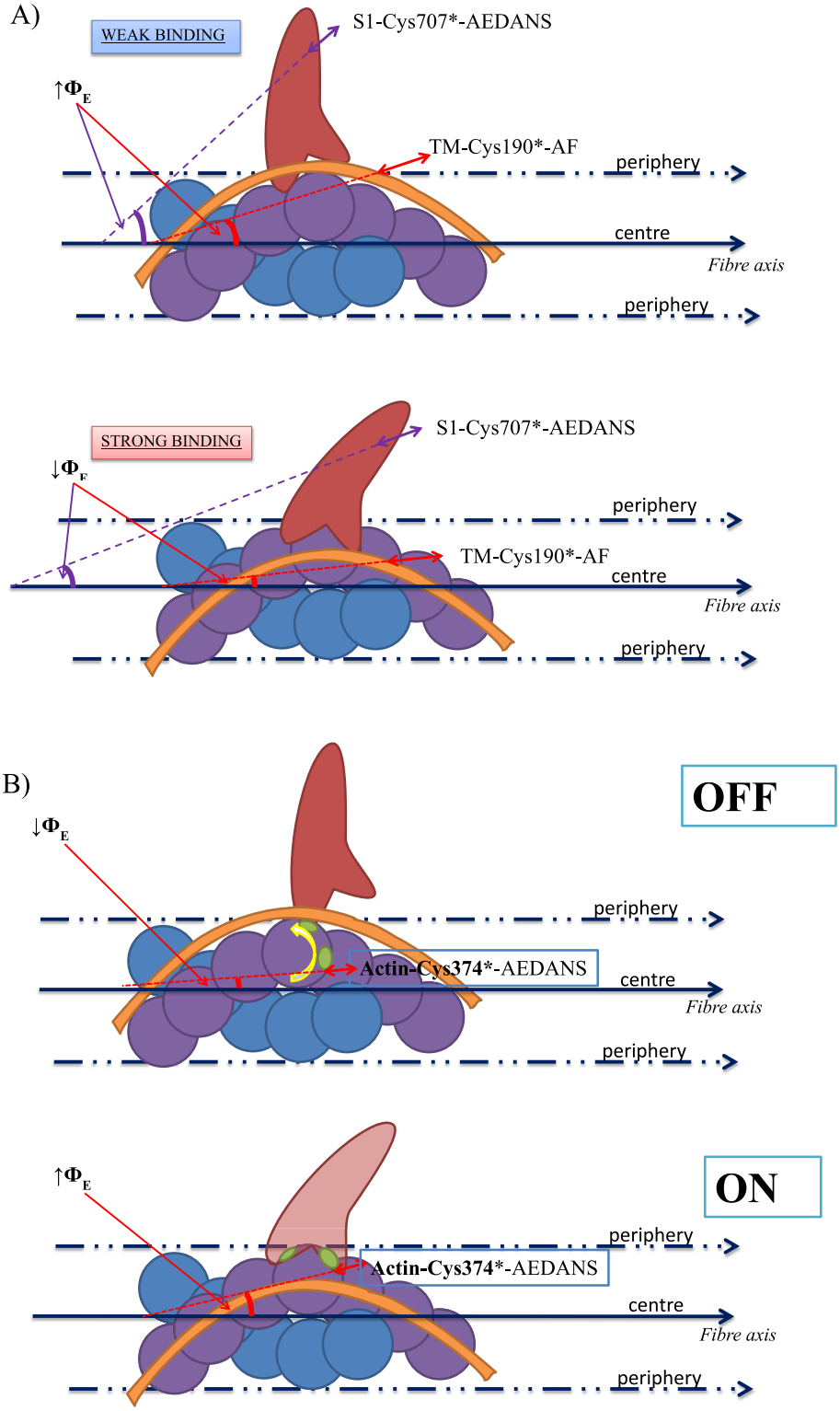

Fig. 2. Cartoons explaining changes in angle Φ_E for S1-AEDANS and TM-AF (A) and actin-AEDANS (B). See explanation in the text. The double-headed arrows reflect the emission dipoles of the probes. Green ovals show myosin-binding sites on actin monomer. Yellow arrow shows a rotation of actin subunit upon activation. (For interpretation of the references to color in this figure legend, the reader is referred to the Web version of this article.)

polarized fluorescence. The $P_{||}$ values were uniformly lower than $P_{\perp}$ values, thus showing that the emission dipoles of IAEDANS were oriented predominantly perpendicular to the fibre axis (Table 1). When the helix plus isotropic model (see Materials and methods) was fitted to the fluorescence polarization data for Ac-AEDANS, the values of the angle Φ_E and $\theta_{1/2}$ were found to be 51° and 6.6°, respectively (Fig. 3a and b). The relative amount of disordered probes (N) did not exceed 0.2, showing a rigid binding of the probes to their target proteins and a highly-ordered arrangement of F-actin in the fibres. Similar values of Φ_E and $\theta_{1/2}$ were obtained earlier [27–29]. Since 1.5-IAEDANS binds covalently to Cys374 in actin subdomain-1, the values of Φ_E (the angle between the filament axis and the emission dipole) and $\theta_{1/2}$ (the

Table 1
The effect of myosin S1 and nucleotides on the polarization ratios, $P_{||}$ and $P_{\perp}$, of 1,5-IAEDANS bound to Cys374 of actin in ghost fibres in the presence of wilt-type tropomyosin (TM-WT), tropomyosin with substitution E240K (TM-E240K) or with substitution R244G (TM-R244G), at simulated stages of ATP hydrolysis cycle. For simulation of few steps of the ATPase cycle the myosin S1, nucleotides of their absence were used.

Nucleotide	S1	TM-WT	TM- E240K	TM- R244G	$P_{||}$ ± SEM	$P_{\perp}$ ± SEM
–	–	+	–	–	0.265 ± 0.004	0.183 ± 0.004
	–	–	+	–	*0.265 ± 0.003	*0.189 ± 0.002
	–	–	–	+	*0.267 ± 0.002	*0.179 ± 0.004
	+	+	–	–	0.198 ± 0.004	0.232 ± 0.004
	+	–	+	–	*0.191 ± 0.003	*0.236 ± 0.002
	+	–	–	+	0.169 ± 0.002	*0.238 ± 0.002
ADP	+	+	–	–	0.184 ± 0.003	0.242 ± 0.002
	+	–	+	–	*0.188 ± 0.003	0.232 ± 0.002
	+	–	–	+	0.157 ± 0.003	*0.243 ± 0.003
AMP-PNP	+	+	–	–	0.210 ± 0.002	0.214 ± 0.002
	+	–	+	–	0.215 ± 0.001	0.199 ± 0.003
	+	–	–	+	0.195 ± 0.002	*0.216 ± 0.003
ATP	+	+	–	–	0.246 ± 0.003	0.181 ± 0.002
	+	–	+	–	*0.249 ± 0.003	0.165 ± 0.003
	+	–	–	+	*0.244 ± 0.003	*0.178 ± 0.003

$P_{||}$ and $P_{\perp}$ ratios were calculated from four intensities of polarized fluorescence, as described in Materials and Methods, in the absence or presence of nucleotides, myosin S1, and TMs. 6–8 ghost fibres were used in the experiments. Error indicates ± SEM. The + and - signs mean the presence or absence nucleotides, S1, and TMs. Unreliable differences are indicated by asterisk (*). The P-values of < 0.05 were accepted as statistically significant.

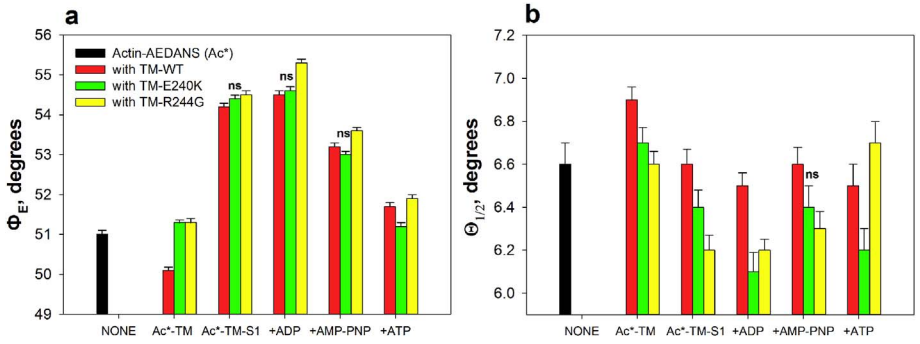

Fig. 3. The values of the angles Φ_E (a) and $\Theta 1/2$ (b) of the polarized fluorescence from 1,5-IAEDANS bound to Cys374 of actin (Actin-AEDANS) in ghost muscle fibres, actin decorated by wild-type tropomyosin (TM-WT; as control) or tropomyosins with substitution E240K (TM-E240K) or R244G (TM-R244G) in the absence or presence S1 and nucleotides ADP, AMP-PNP, and ATP. Φ_E is the angle between the emission dipole of the probe and the filament axis; $\Theta 1/2$ is the angle between the filament axis and muscle fibre axis (see Materials and Methods). The data represent means of 6–8 ghost fibres for each experimental condition (see Table 1). Statistically insignificant changes ($P < 0.05$), compared with the results of the control group, are indicated by "ns".

flexural rigidity) contain information about spatial arrangement and flexibility of the filament.

It is believed that among pure actin filaments there are two actin populations that have different structural and functional properties: those that are favorable for the activation of the ATPase of the myosin heads (constituted by the switched ON monomers) and those that are non-activating (consisting from the switched OFF monomers). These two actin populations are in equilibrium. Myosin, tropomyosin, and troponin (in the Ca^{2+}-dependent manner) are able to shift this balance to increase or decrease the relative amount of the switched ON actin monomers [29–31]. According to the published data [29], attachment of wild type Tpm1.1 to F-actin causes a change of a certain number of actin monomers from "ON" to "OFF" structural state. In other words, an increased number of actin monomers loses the ability to activate the myosin ATPase [32]. It is suggested that the change is accompanied by actin subdomain-1 rotation toward the centre of thin filament, that leads to a decrease of Φ_E and increase of $\theta_{1/2}$ angles of 1,5-IAEDANS bound covalently with Cys374 of actin subdomain-1 [29].

According to Fig. 3a, the binding of wild-type tropomyosin (TM-WT) to Ac-AEDANS decreases the Φ_E angle from 51^0 to 50.1^0 ($P < 0.05$) and increases actin filament flexibility ($\theta_{1/2}$) by ~4% ($P < 0.05$). As indicated above, such changes correlate with both the reduction of the proportion of the switched "ON" actin monomers in F-actin and the transition of actin monomers to "OFF" structural state [29]. In contrast to TM-WT, the E240K and R244G tropomyosins increased slightly the Φ_E value for Ac-AEDANS, probably inhibiting the ON-OFF transition. The flexibility of actin filament in the presence of TM-R244G or TM-E240K slightly decrease (Fig. 3b). Consequently, the wild-type tropomyosin decreased the relative amount of switched ON actin monomers, which is accompanied by a decrease in the angle of Φ_E for Ac-AEDANS (Fig. 3a). This can be explained by a shift in the equilibrium toward a decrease in the activated filaments [29]. On the contrary, the mutant tropomyosins slightly increased the relative amount of switched ON actin monomers.

It is known that the addition of myosin-ADP or rigor myosin to actin increases the relative amount of the switched ON actin monomers [30], which is accompanied by an increase in the angle Φ_E [26]. Our data showed that attachment of S1 to Ac-AEDANS increased the angle Φ_E by 4.1^0 and $\theta_{1/2}$ by 0.3^0 ($P < 0.05$) in the presence of TM-WT (Fig. 3), which switched ON certain amount of actin monomers. This reflects the formation of a strong form of binding between actin and myosin heads. Increasing the Φ_E angle for Ac-AEDANS, decorated by tropomyosin with the substitutions E240K and R244G, amounted to 3.1^0 (by ~ 25% less than in the control). The latter was probably due to the fact that the presence of substitutions in tropomyosin affected the relative amount of switched ON actin monomers [32]. These data do not contradict previous observations [15] showing that the mutations inhibit tropomyosin's ability for cooperative activation of F-actin. The E240K and R244G mutations most likely increase the amount of the switched ON actin monomers in the absence of S1. In the presence of the myosin heads and in the absence of nucleotides the values for Φ_E are somewhat higher and $\theta_{1/2}$ are lower than for control tropomyosin (Fig. 3).

A similar conclusion was reached in the experiments with MgADP bound to S1. In the presence of MgADP the values of Φ_E and $\theta_{1/2}$ were higher by 0.8^0 and lower by 0.3^0 ($P < 0.05$) for the R244G mutant tropomyosin, compared to control tropomyosin (Fig. 3a). That may reflect an increase in the relative number of myosin heads that are in the strong-binding state [30].

In the presence of MgATP the value of Φ_E for Ac*-TM-E240K was lower than for Ac*-TM-WT (the Φ_E value for Ac*-TM-E240K were lower by 0.5^0 ($P < 0.05$), than for Ac*-TM-WT, Fig. 3a). This means that in the presence of TM-E240K the proportion of switched OFF monomers in F-actin in the presence of MgATP was slightly higher than in the presence of TM-WT. In contrast, under similar conditions there was small difference between Ac*-TM-R244G and Ac*-TM-WT (Fig. 3).

Thus, in the absence of myosin, the E240K and R244G mutant tropomyosins shift towards the blocked position and inhibit the switching of actin monomers OFF (this effect is higher for R244G then for E240K). When modeling the different intermediate states of the ATPase cycle, the mutants increased the relative amount of activated actin monomers (except for the mutation R240G in the presence of MgAMP-PNP or MgATP). That may reflect an increase in the relative number of myosin heads that are in the strong-binding state [30]. It can be expected that such changes in the functional state of the filament can affect both the rate of ATP hydrolysis and the elementary steps of the cross-bridge cycle (delete).

3.2. The effects of E240K and R244G substitutions on spatial arrangement and flexibility of tropomyosin on actin filaments

Consistent with our earlier findings [28,29,33,34], the binding of 5-IAF-labeled recombinant TM (AF-TM) to F-actin into ghost fibres initiated polarized fluorescence. The $P_{||}$ values were lower than $P_{\perp}$ values thus showing that the emission dipoles of 5-IAF are predominantly perpendicular to the fibre axis (Table 2).

Earlier we have shown that tropomyosin movement over actin domains is described more precisely, if the values of corrected angle Φ_E ($\Phi_{E\ corr.}$), which take into account the values of Φ_E for Ac-AEDANS obtained under similar experimental conditions, are used for tropomyosin [28,33,35]. In the present study we also introduced similar corrections to the values of Φ_E for TM-AF (WT, E240K, and R244G).

As shown in Fig. 4a, in the absence of S1 and nucleotides the value of $\Phi_{E\ corr.}$ for TM-WT-AF is 55.8°. Under the same conditions the R244G tropomyosin had slightly increased values of $\Phi_{E\ corr.}$ (by 0.3^0, $P < 0.05$) as compared to the wild-type tropomyosin (in the case of E240K-TM the changes were not significant). In our previous works [28,34] and here (Fig. 4a) the character of the changes in the $\Phi_{E\ corr.}$ value for 5-IAF-labeled tropomyosin was considered as being correlated with the azimuthal shift of tropomyosin strands observed in electron microscopy studies of the regulation of the actin-myosin interaction by tropomyosin [36]. An increase in the $\Phi_{E\ corr.}$ value was correlated with the azimuthal shift of tropomyosin strands towards the outer domain of actin, while a decrease in this value with the shift of tropomyosin to the inner domain of actin. According to our data (Fig. 4a), the $\Phi_{Ecorr.}$ values for all tropomyosins were very similar, showing that tropomyosins located near the closed position [37].

The E240K mutant tropomyosin proved to be more rigid in comparison with the wild type tropomyosin (the value of $\theta_{1/2}$ was lower for E240K by 0.6^0, $P < 0.05$). The $\theta_{1/2}$ values for the wild-type and R244G mutant tropomyosins did not differ from each other (Fig. 4b), showing similar flexibility of these tropomyosins in the filaments.

S1 binding to F-actin containing the wild-type or the mutant tropomyosins led to the essential decrease in the $\Phi_{E\ corr}$ and $\theta_{1/2}$ values (Fig. 4). For wild type-TM the values of $\Phi_{E\ corr.}$ decreased by 3.2^0 (from 55.8^0 to 52.6^0; $P < 0.05$), while the changes in $\Phi_{E\ corr.}$ for E240K or R244G tropomyosin were decreased by 3.7^0 (from 55.9^0 to 52.2^0or from 56.1^0 to 52.4^0, respectively; $P < 0.01$) (Fig. 4a). According to the previously published data [28,33] such difference suggested that S1 binding to the thin filament moved tropomyosin mutants further toward the inner domain of actin than TM-WT. In the presence of MgADP, simulating strong-binding state between actin and myosin S1, the value of $\Phi_{E\ corr.}$ was increased by 0.2^0 (from 52.6^0 to 52.8^0; $P < 0.05$) for TM-WT and by 0.4^0 for TM-E240K (from 52.2^0 to 52.6^0; $P < 0.05$), while $\Phi_{E\ corr.}$ for TM-R244G was decreased by 0.2^0 (from 52.4^0 to 52.2^0; $P < 0.05$). Addition of MgAMP-PNP, a non-hydrolysable analog of ATP, to this model system did not cause any significant changes in the values of $\Phi_{E\ corr.}$ (data not shown).

In contrast, in the presence of MgATP, simulating the weak-binding state of actomyosin [32,38], there were differences among the values of $\Phi_{E\ corr.}$ for TM-AF, TM-E240K and TM-R244G, which increased by 2.0^0, 2.4^0, and 1.0^0, respectively (from 52.6^0 to 54.6^0, from 52.2^0 to 54.6^0, and from 52.4^0 to 53.4^0, respectively; $P < 0.05$). Analyzing these data we can assume that both the E240K and R244G break tropomyosin's ability to move toward the outer domain of actin during the ATPase cycle. The ability of tropomyosin to shift to the outer actin domain was suggested earlier by electron microscopy [37]. It is possible that abnormal positions of E240K and R244G tropomyosins is one of the reasons for an increased amount of strongly-bound myosin heads during the simulated stages of the ATPase cycle (see below).

As shown in Fig. 4b, the values of $\theta_{1/2}$, reflecting flexibility of tropomyosin, were not significantly different between TM-E240K and TM-WT (except the stage Ac-TM* where the flexibility of TM-E240K was lower than the flexibility of TM-WT), while the difference between TM-R244G and TM-WT was significant (except the stage Ac-TM*, where significant difference between the values of these tropomyosins was not found). In contrast, in the presence of S1 and nucleotides R244G

Table 2
The effect of myosin S1 and nucleotides on the polarization ratios, $P_{||}$ and $P_{\perp}$, of 5-IAF bound to Cys190 of wild-type tropomyosin (TM-WT), tropomyosin with substitution E240K (TM-E240K) or with substitution R244G (TM-R244G) on the actin filaments in ghost fibres in the absence or presence of myosin heads (S1) and nucleotides (ADP, AMP-PNP, ATP).

Nucleotide	S1	TM-WT	TM-E240K	TM-R244G	$P_{||}$ ± SEM	$P_{\perp}$ ± SEM
–	–	+	–	–	0.130 ± 0.001	0.206 ± 0.002
	–	–	+	–	0.107 ± 0.001	*0.202 ± 0.002
	–	–	–	+	0.123 ± 0.001	0.212 ± 0.001
	+	+	–	–	0.104 ± 0.002	0.198 ± 0.001
	+	–	+	–	0.093 ± 0.001	0.195 ± 0.001
	+	–	–	+	*0.105 ± 0.002	0.223 ± 0.001
ADP	+	+	–	–	0.095 ± 0.001	0.159 ± 0.001
	+	–	+	–	*0.094 ± 0.001	0.162 ± 0.001
	+	–	–	+	0.099 ± 0.002	0.185 ± 0.001
AMP-PNP	+	+	–	–	0.099 ± 0.002	0.140 ± 0.001
	+	–	+	–	*0.099 ± 0.001	*0.142 ± 0.001
	+	–	–	+	0.108 ± 0.002	0.168 ± 0.001
ATP	+	+	–	–	0.118 ± 0.003	0.200 ± 0.002
	+	–	+	–	0.098 ± 0.003	0.226 ± 0.003
	+	–	–	+	0.112 ± 0.002	0.231 ± 0.003

$P_{||}$ and $P_{\perp}$ ratios were calculated from four intensities of polarized fluorescence, as described in Materials and Methods, in the absence or presence of nucleotides, myosin S1, and TMs. 6–8 ghost fibres were used in the experiments. Error indicates ± SEM. The + and - signs mean the presence or absence nucleotides, S1, and TMs. Unreliable differences are indicated by asterisk (*). The P-values of < 0.05 were accepted as statistically significant.

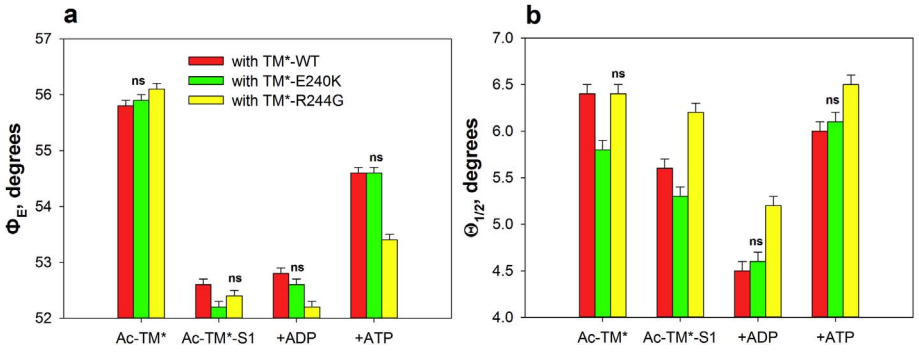

Fig. 4. The values of the angles Φ_E (a) and Θ1/2 (b) of the polarized fluorescence from 5-IAF bound to Cys190 of the Tpm1.1 tropomyosins (WT/E240K/R244G) (TM-AF) on F-actin in the absence or presence S1 and nucleotides, ADP, AMP-PNP, and ATP. Φ_E is the angle between the emission dipole of the probe and the filament axis; Θ1/2 is the angle between the filament axis and muscle fibre axis (see Materials and Methods). The data represent means of 6–8 ghost fibres for each experimental condition (see Table 2). Statistically insignificant changes ($P < 0.05$), compared with the results of the control group, are indicated by "ns".

tropomyosin strands showed greater flexibility than TM-WT.

Thus, in the absence of myosin, both mutations in tropomyosin slightly shift the tropomyosin strands to the outer domain of actin. Conversely, at modeling of the strong-binding of myosin to actin (in the presence of MgADP or in the absence of nucleotides), both mutations cause a noticeable shift of tropomyosin strands to the inner domain of actin. In the presence of MgATP, the displacement of tropomyosin to the inner domain of actin was detected only for the R244G tropomyosin. The position of the E240K mutant tropomyosin did not differ from that of the wild type tropomyosin under these conditions.

3.3. The effects of the substitutions E240K and R244G in tropomyosin on spatial arrangement and mobility of myosin subfragment-1

In line with our earlier findings [28,29,33], the binding of 1,5-IAEDANS-labeled S1 (AEDANS-S1) to F-actin initiated polarized fluorescence. The $P_{||}$ values were higher than $P_{\perp}$ values thus showing that the emission dipoles of 5-IAF was predominantly parallel to the fibre axis (Table 3). The relative amount of disordered probes (N) did not exceed 0.30 for S1-AEDANS, showing a rigid binding of the probes to their target proteins and a highly-ordered arrangement of S1 in the fibres. This allowed studying effects of substitutions introduced in the C-terminal region of skeletal tropomyosin on orientations of the myosin heads and their binding to F-actin during the ATPase cycle. The absence of nucleotides mimicked the AM state of the actomyosin complex. MgADP, MgAMP-PNP, and MgATP were used for mimicking intermediate states of actomyosin, AMˆ·ADP, AM*·ADP, and AM**·ADP·Pi, respectively [24,39], where A is actin and M, Mˆ, M* and M** are various conformational states of the myosin head. As the proteins of muscle system seem to be in a rapid dynamic equilibrium [40], the intermediate states described here in fact may be representatives of different mixtures of a smaller number of sub-states with one of the sub-states prevailing. As it was impossible to resolve the mixture of sub-states in our steady-state experiments, we assumed that in the absence of nucleotides and in the presence of MgADP, MgAMP-PNP or MgATP the strong-binding and weak-binding states were simulated [29].

It was shown earlier that addition of tropomyosin, troponin ± Ca^{2+} and mutations in tropomyosin can shift the dynamic equilibrium between the intermediate states of actomyosin [40] towards predominant formation of the strong-binding or weak-binding conformational states [29,33]. Here we have obtained such an effect. The E240K and R244G mutant tropomyosins shift the equilibrium in a way that favors the formation of the strong-binding conformation states during the ATPase cycle.

According to Fig. 5a, the values of Φ_E and the proportion of randomly oriented fluorophores N (see Material and methods) for S1-AEDANS in the absence or presence of each variant of tropomyosin (TM-WT, TM-E240K, and TM-R244G) during simulated stages of ATP hydrolysis cycle were different. The value of Φ_E for S1-AEDANS in its complex with F-actin formed in the absence of tropomyosin and nucleotides (simulated strong binding, AM state) was close to 43.3^0. Attachment of TM-WT to the decorated F-actin caused a small reduction in Φ_E by 0.3^0 (from 43.3^0 to 43.0^0; $P < 0.05$), while TM-E240K and TM-R244G decreased the angle by 0.6^0 and 0.4^0 ($P < 0.05$), respectively (from 43.3^0 to 42.7^0 and to 42.9^0). At the same time the proportion of randomly oriented fluorophores bound to S1 (N) was also significantly changed in the presence of TM-WT (an increase by 0.013 rel.ative u.nits), but it was even more increased (by 0.033 and 0.044 rel. u., $P < 0.05$) in the presence of TM-E240K and TM-R244G. Thus, all tropomyosins markedly affected the values of Φ_E and N. Such changes in Φ_E and N parameters can be interpreted as an increase in the amount of the strongly bound myosin heads (a rise in the proportion of the

Table 3
The polarization ratios ($P_{||}$ and $P_{\perp}$) of 1,5-IAEDANS bound to Cys707 of myosin S1 on actin filaments in the absence and presence of nucleotides (ADP, AMP-PNP, or ATP), tropomyosins of wild-type (TM-WT) and with substitution E240K (TM-E240K) or R244G (TM-R244G).

Nucleotide	TM-WT	TM- E240K	TM-R244G	$P_{\|\|}$ ± SEM	$P_{\perp}$ ± SEM
-	–	–	–	0.394 ± 0.001	−0.043 ± 0.004
	+	–	–	0.400 ± 0.002	−0.038 ± 0.004
	–	+	–	0.408 ± 0.001	−0.029 ± 0.002
	–	–	+	*0.404 ± 0.002	−0.018 ± 0.004
ADP	+	–	–	0.417 ± 0.004	−0.002 ± 0.004
	–	+	–	0.427 ± 0.001	−0.016 ± 0.005
	–	–	+	0.435 ± 0.002	−0.035 ± 0.004
AMP-PNP	+	–	–	0.395 ± 0.004	0.049 ± 0.005
	–	+	–	*0.396 ± 0.005	0.033 ± 0.005
	–	–	+	0.414 ± 0.004	0.013 ± 0.004
ATP	+	–	–	0.375 ± 0.006	0.128 ± 0.006
	–	+	–	0.414 ± 0.006	0.013 ± 0.006
	–	–	+	*0.383 ± 0.005	0.114 ± 0.004

$P_{||}$ and $P_{\perp}$ ratios were calculated from four intensities of polarized fluorescence, as described in Materials and Methods, in the absence or presence of nucleotides, and TMs. 6–8 ghost fibres were used in the experiments. Error indicates ± SEM. The + and - signs mean the presence or absence nucleotides and TMs. Unreliable differences are indicated by asterisk (*). The P-values of < 0.05 were accepted as statistically significant.

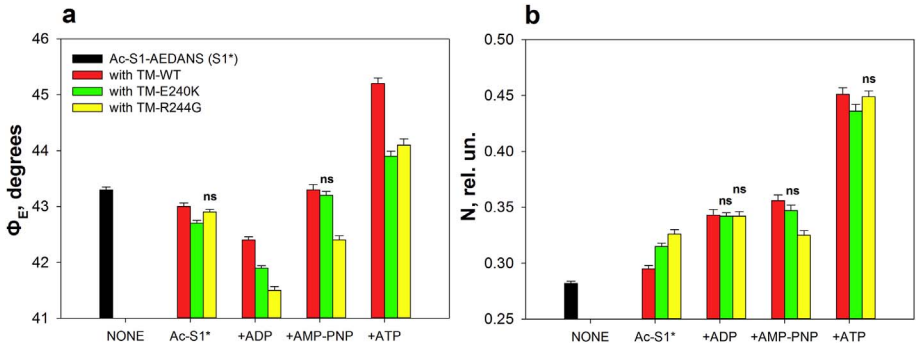

Fig. 5. The values of the angles Φ_E (a) and N (b) of the polarized fluorescence from 1.5-IAEDANS bound to Cys707 of myosin S1 (S1-AEDANS) on F-actin in the absence or presence of TM-WT, TM-E240K or TM-R244G, and nucleotides (ADP, AMP-PNP, or ATP). Φ_E is the angle between the emission dipole of the probe and the filament axis; N is number of disorderly oriented fluorophores (see Materials and Methods). The data represent means of 6–8 ghost fibres for each experimental condition (see Table 3). Statistically insignificant changes ($P < 0.05$), compared with the results of the control group, are indicated by "ns".

myosin heads in conformations corresponding to the AM and/or AM^·ADP states) in the ghost muscle fibres [29]. As mutations in tropomyosin caused an increase in the changes of the polarization fluorimetry parameters, it can be assumed that the mutations increased the amount of the myosin heads in the strong-binding conformation (in the AM and/or AM^·ADP state).

At simulating the strong-binding state of actomyosin in the presence of MgADP (AM^·ADP state), Φ_E and N values for S1-AEDANS on F-actin-TM-WT filaments were decreased by 0.6^0 (from 43.0^0 to 42.4^0; $P < 0.05$) and increased by 0.048 rel. u. (from 0.295 to 0.343; $P < 0.05$), respectively, while for S1-AEDANS on F-actin-TM-E240K and F-actin-TM-R244G the angle of Φ_E was decreased by 0.8^0 (from 42.7^0 to 41.9^0; $P < 0.05$) and 1.4^0, respectively (from 42.9^0 to 41.5^0; $P < 0.05$). The values of N increased by 0.027 (from 0.315 to 0.342; $P < 0.05$) and by 0.016 (from 0.326 to 0.342; $P < 0.05$) for F-actin-TM-E240K and F-actin-TM-R244G (Fig. 5). Since under the influence of MgADP the decrease in the parameter Φ_E was larger and the increase in the parameter N smaller in the presence of the mutant tropomyosins than withthe wild type tropomyosin, it can be assumed that the mutations in tropomyosin promoted the formation of AM^·ADP state (e.i. the amount of actomyosin in AM^·ADP state was larger than in the presence of the wild type tropomyosin). The appearance of myosin heads strongly bound to F-actin at mimicking of AM*·ADP and AM**·ADP·Pi states (in the presence of MgAMP-PNP and MgATP) can be assumed. Indeed, in the presence of the mutant tropomyosins the values of Φ_E and N were lower than in the presence of the wild-type tropomyosin (Fig. 5).

Consequently, in the muscle fibre containing the mutant tropomyosin the relative number of the myosin heads strongly bound to actin was increased [29].

As it has been shown in previous studies [28,29,41], when the MgADP is replaced by MgATP (see Material and Methods) a decrease in the amount of the myosin heads strongly bound to F-actin takes place. According to Fig. 5, the values of Φ_E and N for the control fibres gradually increased when MgADP was replaced by MgATP (mimicking a transition from AM^·ADP to AM**·ADP·Pi state): Φ_E and N increased by 0.9^0 and 0.013 rel. u. ($P < 0.05$) in the presence of MgAMP-PNP and by 2.8^0 and 0.198 rel. u. ($P < 0.05$) in the presence of MgATP. Despite such changes in the presence of E240K and R244G tropomyosins the rise in the values of Φ_E and N was lower than for the control group. The increase in the parameters for S1-AEDANS in the presence of TM-E240K and TM-R244G, respectively, was by 2^0 and 2.6^0 for Φ_E (from 41.9^0 to 43.9^0 and from 41.5^0 to 44.1^0; $P < 0.05$) and by 0.094 and 0.107 rel. u. for N (from 0.436 to 0.342 rel. u. and from 0.449 to 0.342 rel. u.; $P < 0.05$).

In our steady-state experimental conditions in the presence of MgATP at each time, most (but not all) of the myosin heads are in the AM**·ATP·Pi conformation, but there are some myosin heads in other intermediate states (for example in the AM or/and AM^·ADP conformation). The relative amount of the latter heads can change under the influence of tropomyosin [29,33]. Accordingly, an increase in the parameters of N and Φ_E in the presence of the mutant tropomyosins may be interpreted as showing a decrease in the amount of the myosin heads in conformation corresponding to the AM**ADP·Pi statedue to an increase in the number of the myosin heads in conformations corresponding to the AM or/and AM^·ADP states.

The above conclusion is in a good agreement with the changes of the N parameter observed in these experiments (Fig. 5b). Since the decrease in the value of N may reflect an increase in the stiffness of the myosin S1 binding to F-actin and/or tropomyosin [34], the decreased values of N for the filaments containing the mutant tropomyosins in the presence of MgAMP-PNP or MgATP (Fig. 5b) can be explained by a decrease in the amount of the myosin heads in the AM*·ADP and AM**·ADP·Pi conformations due to an increase in the proportion of the myosin heads in the AM or AM^·ADP conformations.

Thus, based on the results obtained in this study, one can suggest that at each simulated stage of the ATPase cycle, the proportion of the myosin heads strongly bound to F-actin is higher in the presence of TM-E240K and TM-R244G, than in the presence of TM-WT.

The mutant tropomyosins can decrease the amplitude of myosin heads (or SH1 helix) tilting during the ATPase cycle (Fig. 5a). The amplitude of change in Φ_E at transition from AM**·ADP·Pi to AM state was lower for the E240K and R244G mutant tropomyosins by 45,5% and 45,5% (decreased from 43.9^0 to 42.7^0 and from 44.1^0 to 42.9^0 for S1-AEDANS in the presence of TM-E240K and TM-R244G, respectively; $P < 0.05$) than for the wild-type tropomyosin (decreased from 45.2^0 to 43.0^0 $P < 0.05$). Since the change in the SH1 helix position seems to be transmitted to the myosin "lever arm" whose rotation is thought to play the key role in the development of force, the decrease of the amplitude of SH1 helix movements in the ATPase cycle indicates that the mutant TMs decrease the efficiency of work of the cross-bridges [42]. The effect of mutations in TM on the amplitude of changes in Φ_E at transition from AM*·ATP to AM state was observed earlier (for example, for the E117K and Q147P mutants) [28,43].

Thus, both mutations increased the relative number of myosin heads, which are in the strongly bound conformation when modeling different stages of the ATP hydrolysis cycle. The higher effect was observed for the R244G mutation. In addition, a reduction in the movement of the myosin SH1 helix (or the myosin heads) during the ATPase cycle was revealed for both mutations.

3.4. The effects of E240K and R244G substitutions in tropomyosin on the actomyosin Mg-ATPase activity

The analysis of the actomyosin Mg-ATPase activity in the presence of TM-WT, TM-E240K and TM-R244G showed that tropomyosins with the substitutions inhibited the actomyosin MgATPase more strongly than wild-type tropomyosin (Fig. 6). The results showed that in the presence of TM-E240K the ATPase was reduced about 1.5-fold more efficiently than in the presence of TM-WT. The inhibition in the presence of TM-R244G was intermediate. The curve obtained by fitting the experimental points to the exponential decay curve demonstrated that

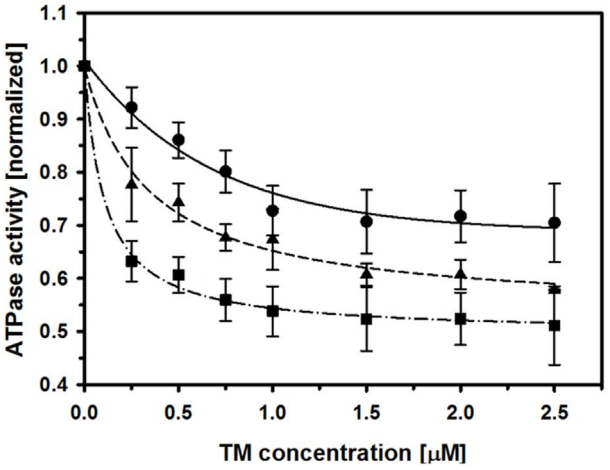

Fig. 6. The effects of the E240K and R244G substitutions in Tpm1.1 on the Mg-ATPase activity of acto-S1. The Mg-ATPase activity was measured in the presence of 7.0 μM F-actin, 0.5 μM S1 and 0–2.5 μM tropomyosin (see Materials and methods). TM-WT (circles), TM-E240K (squares) and TM-R244G (triangles). The lines were obtained by fitting the experimental points to exponential decay in SigmaPlot 12.5.

the maximal inhibition of the ATPase activity was reached at 1.0 μM TM-WT and 1.5 μM TM-E240K. In the presence of TM-R244G the inhibition leveled off at tropomyosin concentrations above 2.5 μM.

To check whether under conditions used in the ATPase assay tropomyosin bound to F-actin, a control actin-binding assay was performed. The results illustrated in Fig. 7 show that both mutant tropomyosins bound weaker to the filament. TM-WT and TM-E240K reached the saturation point at concentrations above 2.5 μM, but TM-R244G did not fully saturate the filament. Thus the more efficient inhibition of the ATPase cannot be correlated with the affinity of mutant tropomyosins to actin, because the high inhibition was achieved with a filament, which was only partially saturated. In turn, lower affinity of mutant tropomyosins can be correlated with the observation that higher concentrations of the mutants were required to reach maximal ATPase inhibition.

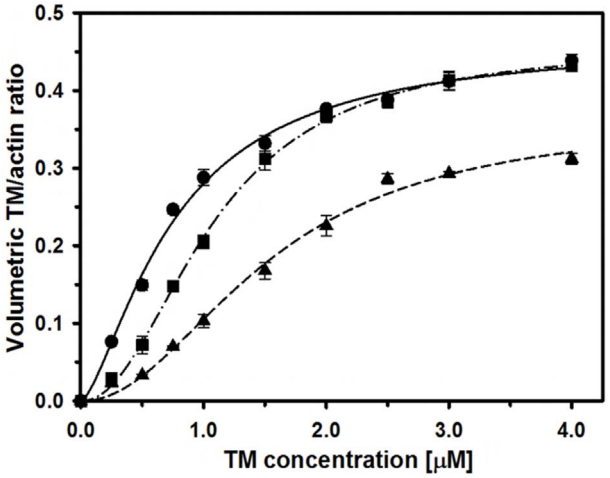

Fig. 7. The effects of the E240K and R244G substitutions on binding of Tpm1.1 to F-actin in the presence of S1-ATP. Binding of TM-WT (circles), TM-E240K (squares) and TM-R244G (triangles) was analyzed by co-sedimentation assay as described in Materials and methods section. The binding curves were obtained by fitting the experimental points to the Hill equation (eq. (1)). Conditions: 7 μM F-actin, 0.5 μM S1, 12 mM Tris-HCl (pH 6.0), 2.5 mM $MgCl_2$, 5 mM KCl, 0.4 mM $CaCl_2$, 2 mM DTT and 2 mM ATP.

4. Discussion

Tropomyosin is a 40-nm long two-chain coiled-coil protein associating head-to-tail to form continuous strands along F-actin, which stabilize the filament and control actin interactions with other proteins. Determination of amino acid sequence and the study of crystal structure of tropomyosin identified periodicities in the structure of the protein. One type of periodicity is presented by ~40 residues pseudo-repeats, which form seven actin-binding sites along the entire length of tropomyosin's molecule. The second type of periodicity is a heptapeptide repeat of residues marked from *a* to *g*. Residues at *a* and *d* positions are hydrophobic and form the core of the coiled-coil, residues at *e* and *g* positions forms salt bridges, stabilizing additionally the protein. Cryo-electron microscopy studies, mutagenesis and computational methods allowed determining residues located in each actin-binding period, mostly in *f* position of the heptad repeat, which are involved in the interaction at actin-tropomyosin interface [4,44–46]. According to F-actin-tropomyosin models, R244 is the consensus site located in the *f* position of the coiled-coil within the seventh actin-binding period of tropomyosin. It interacts electrostatically with D25 exposed on the surface of actin subunit [4,45]. Alterations in the number of electrostatic contacts between the two proteins are believed to play a key role during tropomyosin's movement over actin cable [4,37]. In connection with these data we can suggest that the substitution of positively charged arginine 244 by nonpolar glycine disrupts the interaction with negatively-charged aspartate 25, which is the reason of weakening of actin-tropomyosin affinity found in the previous study [15].

Although E240 is not at the tropomyosin-actin interface [4,45], the E240K substitution also reduces tropomyosin affinity for actin, which suggests that this mutation must affect interactions with actin through a different mechanism than R244G. According to the widely discussed model of *Gestalt*-binding, tropomyosin pre-shapes to fit to F-actin surface [37,47]. Such transformation might introduce particular tension into the rigid structure of tropomyosin. Studies on functions of tropomyosin, which harbors mutations associated with different congenital myopathies, has shown that one of the effects is changed flexibility of tropomyosin on F-actin [28,33,34,41,48,49]. It is possible that many substitutions in tropomyosin alter the pre-shaping process which is manifested in poor affinity for F-actin. An alternative explanation can be deduced from the near atomic resolution structure of full-length tropomyosin molecule [50]. Taking into account the localization of both residues it becomes clear that the side chains of E240 and R244 are exposed on the same face of tropomyosin with their oppositely charged groups being in a close proximity (Fig. 8A). This electrostatic interaction most probably destabilizes the correct orientation of the residue R244, which is required for binding of tropomyosin to actin with high affinity. Hence, reversal of charge caused by the substitution E240K might affect the interactions of tropomyosin with F-actin in a way similar to the substitution R244G, which neutralizes the negative charge of R244.

As follows from our data (Figs. 3–5), the myosin heads shift the strands of the E240K and R244G mutant tropomyosins further into the open position compared to the displacement of the wild-type tropomyosin under similar experimental conditions. The mutant tropomyosins significantly increase the relative amount of actin monomers in the “switched on” conformation (Fig. 3), i.e. in the conformation at which actin is able to activate the hydrolysis of ATP and to bind strongly to myosin. This may result in an increase in the relative number of the myosin heads that, after the nucleotide release, have passed into conformation of the strong-binding to actin (AM and/or AM^·ADP state), even in a solution containing MgATP. In the presence of MgATP, the relative number of the myosin heads in conformation corresponding to the AM**·ADP·Pi state may appear to be decreased because of the increase in the number of heads in conformations corresponding to AM or AM^·ADP states.

It was previously shown that wild-type tropomyosin increases the

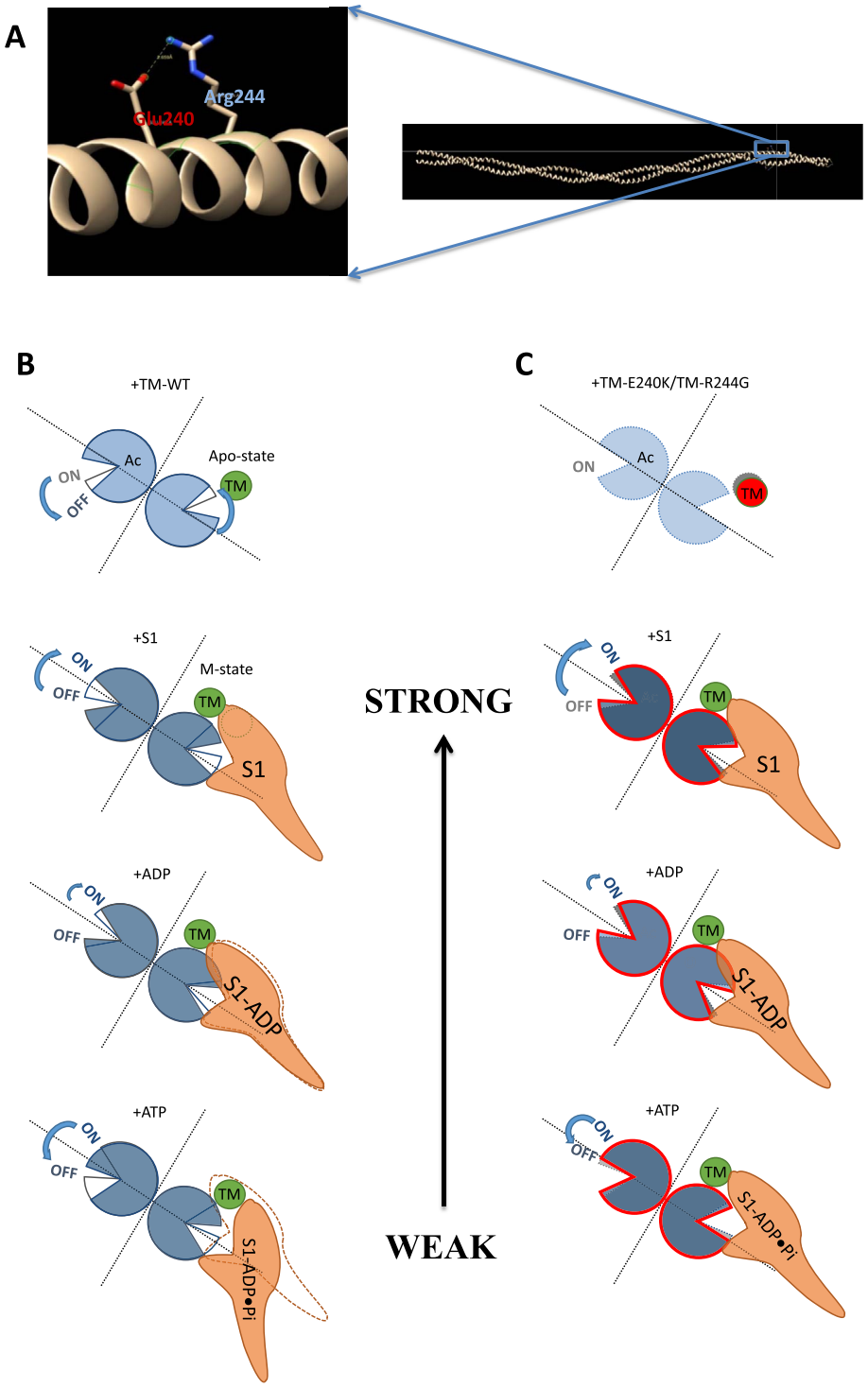

Fig. 8. Localization of E240 (Glu240) and R244 (Arg244) residues in tropomyosin (**A**); the figures were generated using Chimera 1.10.1, based on the Whitby-Phillips structure of Tpm1.1 (PDB: 1C1G) [49]. Models of actin-myosin complex in the presence of TM-WT (**B**), TM-R244G or TM-E240K (**C**) during simulated stages of actomyosin transformation (front view). "Ac", "TM" and "S1" are actin, tropomyosin and myosin subfragment-1, respectively. Unfilled figures in **B** show a state before adding new element to modeled system; grey-filled figures in **C** show the positions of actin, myosin S1 wild-type tropomyosin, illustrated in **B.** The models don't illustrate the exact values of changes, but shows the directions of the changes.

relative amount of both the switched on actin monomers and the myosin heads in the strong-binding conformation when modeling the strong binding of the myosin heads to actin, compared to bare actin filaments [29,33]. However, at mimicking the weak-binding conformation (in the presence of MgATP), the relative number of the myosin heads in conformations corresponding to the AM**·ADP·Pi state was increased in the presence of the wild-type TM. Since there is reason to believe that tropomyosin binds to the myosin head and actin in the absence of nucleotide [51], it has been suggested that binding of myosin to wild-type tropomyosin shifts the latter to the open position (M-position) and is accompanied by an increase in the relative number of the myosin heads in the strongly-bound conformation and actin monomers in the switched on conformation. In the presence of MgATP, wild-type tropomyosin shifts to the closed position and most of the actin

monomers are switched off (the OFF state of F-actin) and the myosin heads are in a weakly bound conformation, since under these conditions the myosin heads under the influence of MgATP are easily transformed into a weakly bound conformation [29,33].

An increase in the relative amount of switched on actin monomers and the appearance of strongly-bound myosin heads in the presence of MgATP was detected only in the presence of the E240K and R244G mutant TMs (Fig. 5). Consequently, these effects are associated with point mutations in tropomyosin. The appearance of an abnormally high number of the myosin heads in the conformation for strong binding to actin appears to result from a decrease in the rate of dissociation of the rigor heads and/or heads containing ADP from actin-tropomyosin, which leads to retention of a fraction of myosin heads in the strong-binding conformation. Thus we suggest that the point mutations in tropomyosin can cause such perturbations in the molecule of this protein, which lead to inhibition of the detachment of the myosin heads in the M and/or M* conformation from tropomyosin and thus increase the relative number of myosin heads in a strongly-bound conformation in a solution containing MgATP.

It is possible that such perturbation in conformations of TM and actin can be one of the reasons of an increase in the amount of the myosin heads in the strong-binding conformations. Further research should verify this assumption. However, it is clear that the abnormal rise in the number of the cross-bridges in AM or AMˆADP conformations, i.e. enhancement of the rate-limiting stages of the ATPase cycle can lead to a decrease in the rate of ATP hydrolysis. Reduction in the rate of ATP hydrolysis by these mutations was previously found in experiments performed in solutions of the proteins [15]. In addition, the abnormal increase in the amount of the myosin heads which are strongly bound to F-actin (of the cross-bridges in the rigor state) may be a reason for the hypo-contractures that are typical for CFTD [52]. However, contracture and weakness of muscle are likely to be a later manifestation of the dysfunction of muscle in CFTD [53]. Therefore, the changes in the conformational states of tropomyosin, actin and myosin at mimicking the different intermediate states of the ATPase cycle cannot directly indicate the relationship of these changes in conformations with the appearance of contractures and weakness of the muscle fibres found in CFTD myopathy.

5. Conclusion

Destabilizing the tropomyosin-actin interface was proposed by other authors as a general mechanism explaining hyper- or hypocontractile phenotypes caused by point mutations in tropomyosin [53–55]. As in the absence of troponin tropomyosin is thought to occupy the closed C-state [5], disruption of specific tropomyosin-actin interactions would destabilize this state. Indeed, a shift of tropomyosin chains towards the open position was observed in this work for both tropomyosin mutants, which should result in more activated filaments. However *in vitro* studies on the mutations R244G in Tpm1.1 (this work and [15]) as well as hypocontractile phenotype observed in myopathy patients carrying an equivalent mutation R245G in Tpm3.12 [10], consistently show alterations in actomyosin interactions.

Based on the experimental data collected in this work we propose models of actin-myosin-tropomyosin contractile system working in the presence of three forms of tropomyosin: TM-WT, TM-E240K and TM-R244G. Schematic illustrations of the models are shown in Fig. 8B and C. According to the models, during the simulation of weak-to-strong transformation in actomyosin both mutant tropomyosins are shifted further to the inner domain of actin, contributing to the exposure of more myosin-binding sites on the actin surface than in the presence of TM-WT. High ratio of myosin heads dwelling in the strongly-bound state restricts the ability of myosin S1 to undergo full cross-bridge cycle. This and previous analyzes of fluorescence polarization of probes attached to actin, myosin head and tropomyosin revealed that hypocontraction caused by alterations in actomyosin interactions have a heterogeneous and complex origin. The hypocontractile phenotype does not depend only on the affinity of tropomyosin for actin, which shifts the equilibrium between different activation states and determines steric blocking of myosin-binding. Alterations in tropomyosin structure also affect the equilibrium between ON/OFF states of actin monomers, quantity and character of the myosin heads binding to TM and the rate of myosin head cycling during ATP hydrolysis [28,33,34].

Compliance with ethics guidelines

Armen O. Simonyan, Vladimir V. Sirenko, Olga E. Karpicheva, Katarzyna Robaszkiewicz, Joanna Moraczewska, Małgorzata Śliwinska, Zoya I. Krutetskaya, and Yurii S.Borovikov declare that they have no conflict of interests.

Acknowledgements

The work was supported by the Russian Science Foundation (Grant Number 17-14-01224) and the statutory funds of Kazimierz Wielki University.

References

[1] D.F.A. Mckillop, M.A. Geeves, Regulation of the interaction between actin and myosin subfragment 1: evidence for three states of the thin filament, Biophys. J. 65 (1993) 693–701.
[2] W. Lehman, R. Craig, Tropomyosin and the steric mechanism of muscle regulation, Adv. Exp. Med. Biol. 644 (2008) 95–109.
[3] R. Desai, M.A. Geeves, N.M. Kad, Using fluorescent myosin to directly visualize cooperative activation of thin filaments, J. Biol. Chem. 290 (2015) 1915–1925.
[4] X. Li, L.S. Tobacman, J.Y. Mun, R. Craig, S. Fischer, W. Lehman, Tropomyosin position on F-actin revealed by EM reconstruction and computational chemistry, Biophys. J. 100 (2011) 1005–1013.
[5] P. Vibert, R. Craig, W. Lehman, Steric-model for activation of muscle thin filaments, J. Mol. Biol. 266 (1997) 8–14.
[6] D.R. Sousa, S.M. Stagg, M.E. Stroupe, Cryo-EM structures of the actin:tropomyosin filament reveal the mechanism for the transition from C- to M-State, J. Mol. Biol. 425 (2013) 4544–4555.
[7] S.E. Hitchcock-Degregori, Tropomyosin: function follows structure, Adv. Exp. Med. Biol. 644 (2008) 60–72.
[8] N.J. Greenfield, Y.J. Huang, G.V.T. Swapna, A. Bhattacharya, B. Rapp, A. Singh, G.T. Montelione, S.E. Hitchcock-DeGregori, Solution NMR Structure of the Junction between Tropomyosin molecules: implications for actin binding and regulation, J. Mol. Biol. 364 (2006) 80–96.
[9] J.J. Frye, V.A. Klenchin, C.R. Bagshaw, I. Rayment, Insights into the importance of hydrogen bonding in the γ-phosphate binding pocket of myosin: structural and functional studies of serine 236, Biochemistry 49 (2010) 4897–4907.
[10] N.F. Clarke, H. Kolski, D.E. Dye, E. Lim, R.L.L. Smith, R. Patel, M.C. Fahey, R. Bellance, N.B. Romero, E.S. Johnson, A. Labarre-Vila, N. Monnier, N.G. Laing, K.N. North, Mutations in TPM3 are a common cause of congenital fiber type disproportion, Ann. Neurol. 63 (2008) 329–337.
[11] M.W. Lawlor, E.T. Dechene, E. Roumm, A.S. Geggel, A.H. Beggs, Mutations of tropomyosin 3 (TPM3) are common and associated with type 1 myofiber hypotrophy in congenital fiber rype disproportion, 31 (2011) 176–183.
[12] S.S. Margossian, S. Lowey, Preparation of myosin and its subfragments from rabbit skeletal muscle, Methods Enzymol. 85 (1982) 55–71.
[13] J.A. Spudich, S. Watt, The regulation of rabbit skeletal muscle contraction, J. Biol. Chem. 246 (1971) 4866.
[14] E.N. Hudson, G. Weber, Synthesis and characterization of two fluorescent sulfhydryl reagents, Biochemistry 12 (1973) 4154–4161.
[15] K. Robaszkiewicz, E. Dudek, A.A. Kasprzak, J. Moraczewska, Functional effects of congenital myopathy-related mutations in gamma-tropomyosin gene, Biochim. Biophys. Acta - Mol. Basis Dis 1822 (2012) 1562–1569.
[16] J.D. Potter, Preparation of troponin and its subnits, Methods Enzymol. 85 (1982) 241–263.
[17] J. Moraczewska, K. Nicholson-Flynn, S.E. Hitchcock-Degregori, The ends of tropomyosin are major determinants of actin affinity and myosin subfragment 1-induced binding to F-actin in the open state, Biochemistry 38 (1999) 15885–15892.
[18] E. Rome, Relaxation of glycerinated muscle: low-angle X-ray diffraction studies, J. Mol. Biol. 65 (1972).
[19] M.I. Khoroshev, I.S. Borovikov, The ghost muscle fiber with thin filaments reconstructed from nonmuscle actin–a model for studying the cytoskeleton using polarization microfluorimetry, Tsitologiya 33 (1991) 76–79.
[20] H.D. White, Special instrumentation and techniques for kinetic studies of contractile systems, Methods Enzymol. 85 (1982) 698–708.
[21] R. Skórzewski, M. Śliwińska, D. Borys, A. Sobieszek, J. Moraczewska, Effect of actin C-terminal modification on tropomyosin isoforms binding and thin filament regulation, Biochim. Biophys. Acta Protein Proteonomics 1794 (2009) 237–243.
[22] Y.S. Borovikov, I.V. Dedova, C.G. dos Remedios, N.N. Vikhoreva, P.G. Vikhorev,

S.V. Avrova, T.L. Hazlett, B.W. Van Der Meer, Fluorescence depolarization of actin filaments in reconstructed myofibers: the effect of S1 or pPDM-S1 on movements of distinct areas of actin, Biophys. J. 86 (2004) 3020–3029.
[23] T. Yanagida, F. Oosawa, Polarized fluorescence from ε-ADP incorporated into F-actin in a myosin-free single fiber: conformation of F-actin and hanges induced in it by heavy meromyosin, J. Mol. Biol. 126 (1978) 507–524.
[24] O. Roopnarine, D.D. Thomas, Orientation of intermediate nucleotide states of indane dione spin-labeled myosin heads in muscle fibers, Biophys. J. 70 (1996) 2795–2806.
[25] M. Lorenz, K.J. Poole, D. Popp, G. Rosenbaum, K.C. Holmes, An atomic model of the unregulated thin filament obtained by X-ray fiber diffraction on oriented actin-tropomyosin gels, J. Mol. Biol. 246 (1995) 108–119.
[26] M. Lorenz, K.J.V. Poole, D. Popp, G. Rosenbaum, K.C. Holmes, An atomic model of the unregulated thin filament obtained by x-ray fiber diffraction on oriented actin-tropomyosin gels, J. Mol. Biol. 246 (1995) 108–119.
[27] Y.S. Borovikov, J. Moraczewska, M.I. Khoroshev, H. Strzelecka-Golaszewska, Proteolytic cleavage of actin within the DNase-I-binding loop changes the conformation of F-actin and its sensitivity to myosin binding, Biochim. Biophys. Acta Protein Struct. Mol. Enzymol. 1478 (2000) 138–151.
[28] O.E. Karpicheva, A.O. Simonyan, N.V. Kuleva, C.S. Redwood, Y.S. Borovikov, Myopathy-causing Q147P TPM2 mutation shifts tropomyosin strands further towards the open position and increases the proportion of strong-binding cross-bridges during the ATPase cycle, Biochim. Biophys. Acta Protein Proteonomics 1864 (2016) 260–267.
[29] Y.S. Borovikov, O.E. Karpicheva, S.V. Avrova, C.S. Redwood, Modulation of the effects of tropomyosin on actin and myosin conformational changes by troponin and Ca2+, Biochim. Biophys. Acta Protein Proteonomics 1794 (2009) 985–994.
[30] A.M. Gordon, E. Homsher, M. Regnier, Regulation of contraction in striated muscle, Physiol. Rev. 80 (2000) 853–924.
[31] Y.S. Borovikov, N.B. Gusev, Effect of troponin-tropomyosin complex and Ca2+ on conformational changes in F-actin induced by myosin subfragment-1, Eur. J. Biochem. 136 (1983) 363–369.
[32] A.M. Gordon, E. Homsher, M. Regnier, Regulation of contraction in striated muscle, Physiol. Rev. 80 (2000) 853–924.
[33] Y.S. Borovikov, S.V. Avrova, N.A. Rysev, V.V. Sirenko, A.O. Simonyan, A.A. Chernev, O.E. Karpicheva, A. Piers, C.S. Redwood, Aberrant movement of β-tropomyosin associated with congenital myopathy causes defective response of myosin heads and actin during the ATPase cycle, Arch. Biochem. Biophys. 577–578 (2015) 13–23.
[34] Y.S. Borovikov, N.A. Rysev, A.A. Chernev, S.V. Avrova, O.E. Karpicheva, D. Borys, M. Śliwińska, J. Moraczewska, Abnormal movement of tropomyosin and response of myosin heads and actin during the ATPase cycle caused by the Arg167His, Arg167Gly and Lys168Glu mutations in TPM1 gene, Arch. Biochem. Biophys. 606 (2016) 157–166.
[35] N.A. Rysev, I.A. Nevzorov, S.V. Avrova, O.E. Karpicheva, C.S. Redwood, D.I. Levitsky, Y.S. Borovikov, Gly126Arg substitution causes anomalous behaviour of α-skeletal and β-smooth tropomyosins during the ATPase cycle, Arch. Biochem. Biophys. 543 (2014) 57–66.
[36] J. von der Ecken, S.M. Heissler, S. Pathan-Chhatbar, D.J. Manstein, S. Raunser, Cryo-EM structure of a human cytoplasmic actomyosin complex at near-atomic resolution, Nature 534 (2016) 724–728.
[37] W. Lehman, M. Orzechowski, X.E. Li, S. Fischer, S. Raunser, Gestalt-Binding of tropomyosin on actin during thin filament activation, J. Muscle Res. Cell Motil. 34 (2013) 155–163.
[38] A.A. Bobkov, E.A. Bobkova, E. Homsher, E. Reisler, Activation of regulated actin by SH1-modified myosin subfragment 1, Biochemistry 36 (1997) 7733–7738.
[39] R.S. Goody, W. Hofmann, Stereochemical aspects of the interaction of myosin and actomyosin with nucleotides, J. Muscle Res. Cell Motil. 1 (1980) 101–115.
[40] M.A. Geeves, The dynamics of actin and myosin association and the crossbridge model of muscle contraction, Biochem. J. 274 (1991) 1–14.
[41] O.E. Karpicheva, P. Robinson, A. Piers, Y.S. Borovikov, C.S. Redwood, The nemaline myopathy-causing E117K mutation in β-tropomyosin reduces thin filament activation, Arch. Biochem. Biophys. 536 (2013) 25–30.
[42] H. Fujita, X. Lu, M. Suzuki, S. Ishiwata, M. Kawai, The effect of tropomyosin on force and elementary steps of the cross-bridge cycle in reconstituted bovine myocardium, J. Physiol 556 (2004) 637–649.
[43] O.E. Karpicheva, C.S. Redwood, Y.S. Borovikov, The E117K mutation in β-tropomyosin disturbs concerted conformational changes of actomyosin in muscle fibers, Arch. Biochem. Biophys. 549 (2014) 12–16.
[44] A. Wagner, The interaction of alpha, alpha- and alpha, beta-tropomyosin with actin filaments, FEBS Lett. 119 (1980) 245–248.
[45] B. Barua, M.C. Pamula, S.E. Hitchcock-DeGregori, Evolutionarily conserved surface residues constitute actin binding sites of tropomyosin, Proc. Natl. Acad. Sci. U. S. A. 108 (2011).
[46] E. Behrmann, M. Müller, P.A. Penczek, H.G. Mannherz, D.J. Manstein, S. Raunser, Structure of the rigor actin-tropomyosin-myosin complex, Cell 150(2012) 327–338.
[47] K.C. Holmes, W. Lehman, Gestalt-binding of tropomyosin to actin filaments, J. Muscle Res. Cell Motil. 29 (2008) 213–219.
[48] M.L. Lynn, L. Tal Grinspan, T.A. Holeman, J. Jimenez, J. Strom, J.C. Tardiff, The structural basis of alpha-tropomyosin linked (Asp230Asn) familial dilated cardiomyopathy, J. Mol. Cell. Cardiol. 108 (2017) 127–137.
[49] W. Zheng, S.E. Hitchcock-DeGregori, B. Barua, Investigating the effects of tropomyosin mutations on its flexibility and interactions with filamentous actin using molecular dynamics simulation, J. Muscle Res. Cell Motil. 37 (2016) 131–147.
[50] F.G. Whitby, G.N. Phillips, Crystal structure of tropomyosin at 7 Ångstroms resolution, Proteins Struct. Funct. Bioinforma 38 (2000) 49–59.
[51] K. Ueda, C. Kimura-Sakiyama, T. Aihara, M. Miki, T. Arata, Calcium-Dependent interaction sites of tropomyosin on reconstituted muscle thin filaments with bound myosin heads as studied by site-directed spin-labeling, Biophys. J. 105 (2013) 2366–2373.
[52] M. Marttila, V.L. Lehtokari, S. Marston, T.A. Nyman, C. Barnerias, A.H. Beggs, E. Bertini, O. Ceyhan-Birsoy, P. Cintas, M. Gerard, B. Gilbert-Dussardier, J.S. Hogue, C. Longman, B. Eymard, M. Frydman, P.B. Kang, L. Klinge, H. Kolski, H. Lochmüller, L. Magy, V. Manel, M. Mayer, E. Mercuri, K.N. North, S. Peudenier-Robert, H. Pihko, F.J. Probst, R. Reisin, W. Stewart, A.L. Taratuto, M. de Visser, E. Wilichowski, J. Winer, K. Nowak, N.G. Laing, T.L. Winder, N. Monnier, N.F. Clarke, K. Pelin, M. Grönholm, C. Wallgren-Pettersson, Hum. Mutat. 35 (2014) 779–790.
[53] S. Marston, M. Memo, A. Messer, M. Papadaki, K. Nowak, E. Mcnamara, R. Ong, M. El-Mezgueldi, X. Li, W. Lehman, Mutations in repeating structural motifs of tropomyosin cause gain of function in skeletal muscle myopathy patients, Hum. Mol. Genet. 22 (2013) 4978–4987.
[54] M. Orzechowski, S. Fischer, J.R. Moore, W. Lehman, G.P. Farman, Energy landscapes reveal the myopathic effects of tropomyosin mutations, Arch. Biochem. Biophys. 564 (2014) 89–99.
[55] S. Donkervoort, M. Papadaki, J.M. de Winter, M.B. Neu, J. Kirschner, V. Bolduc, M.L. Yang, M.A. Gibbons, Y. Hu, J. Dastgir, M.E. Leach, A. Rutkowski, A.R. Foley, M. Kruger, E.P. Wartchow, E. McNamara, R. Ong, K.J. Nowak, N.G. Laing, N.F. Clarke, C.A.C. Ottenheijm, S.B. Marston, C.G. Bönnemann, TPM3 deletions cause a hypercontractile congenital muscle stiffness phenotype, Ann. Neurol. 78 (2015) 985–994.